

SPREAD OPTION PRICING USING ADI METHODS

VIDA HEIDARPOUR-DEHKORDI AND CHRISTINA C. CHRISTARA

Abstract. Spread option contracts are becoming increasingly important, as they frequently arise in the energy derivative markets, e.g. exchange electricity for oil. In this paper, we study the pricing of European and American spread options. We consider the two-dimensional Black-Scholes Partial Differential Equation (PDE), use finite difference discretization in space and consider Crank-Nicolson (CN) and Modified Craig-Sneyd (MCS) Alternating Direction Implicit (ADI) methods for timestepping. In order to handle the early exercise feature arising in American options, we employ the discrete penalty iteration method, introduced and studied in Forsyth and Vetzal (2002), for one-dimensional PDEs discretized in time by the CN method. The main novelty of our work is the incorporation of the ADI method into the discrete penalty iteration method, in a highly efficient way, so that it can be used for two or higher-dimensional problems. The results from spread option pricing are compared with those obtained from the closed-form approximation formulae of Kirk (1995), Venkatramanan and Alexander (2011), Monte Carlo simulations, and the Brennan-Schwartz ADI Douglas-Rachford method, as implemented in MATLAB. In all spread option test cases we considered, including American ones, our ADI-MCS method, implemented on appropriate non-uniform grids, gives more accurate prices and Greeks than the MATLAB ADI method.

Key words. Modified Craig-Sneyd, alternating direction implicit method, two-dimensional Black-Scholes, American option, spread option, exchange option, analytical approximation, numerical PDE solution, and penalty iteration.

1. Introduction

Spread options are popular financial contracts for which, except the simplest case called *exchange contracts* (i.e. strike = 0), there exist no analytical solutions. We are interested in pricing spread options, using a numerical Partial Differential Equation (PDE) approach.

A spread option is a two-asset derivative, whose payoff depends on the difference between the prices $s_1(t)$ and $s_2(t)$ of the two assets. Essentially, the European call (put) spread option gives the holder the right, but not the obligation, to buy (sell) the spread $s_1(T) - s_2(T)$ at the exercise price K , at maturity time T .

In the energy markets, an example of a spread option is an option on the *spark spread*, which is the difference between the price received by a generator for electricity produced and the cost of the natural gas needed to produce that electricity. Another example of a spread option is an option on the *crack spread*, which is the difference between the price of refined petroleum products and crude oil.

Several spread option pricing approaches can be used, such as Monte Carlo (MC) simulations or tree (lattice) methods, however, for problems in low dimensions, the PDE approach is a popular choice, due to its efficiency and global character. In addition, the essential parameters for risk-management and hedging of financial derivatives, such as delta and gamma, are generally much easier to compute via the PDE approach than via other methods.

We consider the basic two-dimensional Black-Scholes (BS) PDE and compute a numerical approximation to the solution using second-order finite differences (FD)

discretization in space and Crank-Nicolson (CN) or Alternating Direction Implicit (ADI) methods, more specifically, the Modified Craig-Sneyd (MCS) method, for timestepping. Note that MCS is stable without stepsize restrictions, and exhibits second-order convergence in both space and time when applied to PDEs with mixed derivative terms ([12], [13], [24]). To price American spread options a non-linear penalty term is added to the PDE, and an iterative method is employed to solve the resulting problem. This technique is introduced in [8] for one-dimensional problems and CN timestepping. Our focus in this paper is to incorporate the ADI-MCS method efficiently into the penalty iteration. We present results from our ADI-MCS method on various types of spread options and compare them to results from other PDE approximation methods, analytical approximation formulae and MC simulation methods.

Regarding analytical formulae, for the case of European exchange options, there exists the *Margrabe* formula [17], which gives the exact price of the exchange option, and is an accurate reference value for comparison. For general European spread options, there is no formula that gives the exact price. However, there exist analytical formulae that approximate the price of European spread options. These approximations include Kirk's formula [15] and the formula developed by Venkatramanan and Alexander [22]. Kirk's formula provides a good approximation of spread option prices when the strike K is small compared to the current value of s_2 . Venkatramanan and Alexander [22] express the price of a European spread option as the sum of the prices of two compound exchange options (CEOs), one to exchange vanilla call options and the other to exchange vanilla put options. Using a conditional relationship between the strike of vanilla options and the implied correlation, the authors reduce the problem to one-dimensional put and call vanilla option computations.

For both European and American spread option test cases, we also consider two different numerical approximations in MATLAB. One is MATLAB's implementation of the Douglas-Rachford (DR) ADI timestepping (func. `spreadsensbyfd`), and another is the MC simulations (func. `spreadsensbyls`). In the MATLAB function `spreadsensbyfd`, for American spread options, the ADI-DR timestepping is combined with the Brennan-Schwartz algorithm [1], in order to solve the Linear Complementarity Problem (LCP) arising when pricing American type options. In [10], the algorithm is re-formulated using a form of LU decomposition, and this form is used in the MATLAB code.

Moreover, we display results of Greeks computed using our method, as well as MATLAB's functions `spreadsensbyfd` and `spreadsensbyls`. Finally, we present results for the free boundary.

In Section 2, we present the PDE along with initial and boundary conditions. The discretization of the problem along the space dimension and the ADI timestepping technique are described in Section 3. In Section 4, the handling of American options using the discrete penalty iteration method for both CN and ADI timestepping is demonstrated. Special attention is paid in efficiently incorporating the ADI-MCS method into the discrete penalty iteration. Finally, in Section 5, we present numerical results that demonstrate the performance of our method. We first compare our results for a European exchange option with Margrabe's exact solution. We then make an experimental investigation on the accuracy and convergence of the price computed by our method for both uniform and non uniform

spatial meshes for different test case scenarios, for which the exact solution is unknown. We also compare with the results obtained by analytical approximation formulae and other numerical methods.

2. Problem Description

Let's assume that the asset prices s_1 and s_2 follow the standard Wiener processes

$$(1) \quad ds_i = (r - q_i)s_i dt + \sigma_i s_i dW_i, \quad i = 1, 2, \quad \text{with } \mathcal{E}[dW_1 dW_2] = \rho dt.$$

Variables σ_1 and σ_2 are the volatilities of s_1 and s_2 , respectively, q_1 and q_2 the dividends paid by s_1 and s_2 , respectively, r the risk-free interest rate, ρ the correlation between s_1 and s_2 , and $\mathcal{E}[\cdot]$ the expectation. It can be shown that under assumption (1), and some other assumptions, the price $u = u(s_1, s_2, \tau)$ of a European option on two correlated assets satisfies the backward BS PDE

$$(2) \quad \frac{\partial u}{\partial \tau} = Lu \equiv \frac{\sigma_1^2 s_1^2}{2} \frac{\partial^2 u}{\partial s_1^2} + \rho \sigma_1 \sigma_2 s_1 s_2 \frac{\partial^2 u}{\partial s_1 \partial s_2} + \frac{\sigma_2^2 s_2^2}{2} \frac{\partial^2 u}{\partial s_2^2} \\ + (r - q_1) s_1 \frac{\partial u}{\partial s_1} + (r - q_2) s_2 \frac{\partial u}{\partial s_2} - ru$$

where τ the backward time variable, i.e. $\tau = T - t$, with t being the forward time variable ($t \in [0, T]$) and T the maturity time of the option.

The initial condition at time $t = T$ ($\tau = 0$), which arises from the option's payoff, for a spread option with exercise price K is

$$(3) \quad u^*(s_1, s_2) = u(s_1, s_2, 0) = [\omega(s_1 - s_2 - K)]^+.$$

The values $\omega = 1$ and $\omega = -1$ indicate scenarios of call and put options, respectively. Throughout this paper, the notation x^+ is defined as $x^+ \equiv \max\{x, 0\}$.

The PDE (2) is defined in a semi-infinite $[0, \infty) \times [0, \infty)$ domain in space. In order to formulate boundary conditions, we truncate the semi-infinite domain to $[0, S_1] \times [0, S_2]$, for large enough values of S_1 and S_2 . The particular values of S_1 and S_2 used in our experiments are given in Section 5. For European spread options, we use the following (Dirichlet) boundary conditions, arising from the payoff with discounting:

$$(4) \quad u(0, s_2, \tau) = [\omega(-s_2 e^{-q_2 \tau} - K e^{-r \tau})]^+,$$

$$(5) \quad u(s_1, 0, \tau) = [\omega(s_1 e^{-q_1 \tau} - K e^{-r \tau})]^+,$$

$$(6) \quad u(S_1, s_2, \tau) = [\omega(S_1 e^{-q_1 \tau} - s_2 e^{-q_2 \tau} - K e^{-r \tau})]^+,$$

$$(7) \quad u(s_1, S_2, \tau) = [\omega(s_1 e^{-q_1 \tau} - S_2 e^{-q_2 \tau} - K e^{-r \tau})]^+.$$

To formulate boundary conditions for American spread options, we consider the boundary conditions (4)-(7) for European options, and take into account that the American option value is always above or on the payoff. Thus, for American spread options, we consider the (Dirichlet) boundary conditions

$$(8) \quad u(0, s_2, \tau) = \max\{[\omega(-s_2 e^{-q_2 \tau} - K e^{-r \tau})]^+, [\omega(-s_2 - K)]^+\},$$

$$(9) \quad u(s_1, 0, \tau) = \max\{[\omega(s_1 e^{-q_1 \tau} - K e^{-r \tau})]^+, [\omega(s_1 - K)]^+\},$$

$$(10) \quad u(S_1, s_2, \tau) = \max\{[\omega(S_1 e^{-q_1 \tau} - s_2 e^{-q_2 \tau} - K e^{-r \tau})]^+, [\omega(S_1 - s_2 - K)]^+\},$$

$$(11) \quad u(s_1, S_2, \tau) = \max\{[\omega(s_1 e^{-q_1 \tau} - S_2 e^{-q_2 \tau} - K e^{-r \tau})]^+, [\omega(s_1 - S_2 - K)]^+\}.$$

It is worth noting that, except for the case $s_1 = 0$ and $\omega = 1$, the above boundary conditions for European and American spread options are approximate. However, our numerical results for the chosen S_1 and S_2 indicate that the inexact boundary conditions do not hinder the accuracy of our methods.

3. PDE Discretization

Let $\tau^k, k = 0, \dots, N_t$, be points in time, with $0 = \tau^0 < \tau^1 < \dots < \tau^{N_t} = T$, and $\Delta\tau^k = \tau^k - \tau^{k-1}, k = 1, \dots, N_t$. Note that $\tau^k, k = 0, \dots, N_t$, may be non-uniformly spaced. Consider a possibly non-uniform partition of $[0, S_1]$ with gridpoints $s_{1,i}, i = 0, \dots, N_x, 0 = s_{1,0} < s_{1,1} < \dots < s_{1,N_x} = S_1$, and a possibly non-uniform partition of $[0, S_2]$ with gridpoints $s_{2,j}, j = 0, \dots, N_y, 0 = s_{2,0} < s_{2,1} < \dots < s_{2,N_y} = S_2$. Let $h_i^x = s_{1,i} - s_{1,i-1}, i = 1, \dots, N_x$, and $h_j^y = s_{2,j} - s_{2,j-1}, j = 1, \dots, N_y$.

Let $u^k = u^k(s_1, s_2)$ be the semi-discrete (CN or ADI timestepping) approximation to the solution of the PDE (2) at time τ^k . Let also $u_{i,j}^k$ be the approximation to the solution of the PDE at point (s_1, s_2, τ^k) , i.e., $u_{i,j}^k \approx u(s_{1,i}, s_{2,j}, \tau^k)$, $i = 1, \dots, N_x - 1, j = 1, \dots, N_y - 1$. Furthermore, let $\mathbf{u}^k = [u_{1,1}^k, u_{2,1}^k, \dots, u_{N_x, N_y}^k]^T$ be the $(N_x - 1)(N_y - 1) \times 1$ vector of values $u_{i,j}^k, i = 1, \dots, N_x - 1, j = 1, \dots, N_y - 1$. Note that the indexing of the components is first along the s_1 -dimension, then along the s_2 -dimension.

3.1. Space discretization. Using standard second-order centered finite differences for the spatial derivatives, the discretization of L of (2) results in a matrix A , which can be written as $A = A_0 + A_1 + A_2$, where A_1 and A_2 are the matrices arising from FD discretization of the first and second derivative terms of (2) with respect to the s_1 - and s_2 variables, respectively, and A_0 is the matrix resulting from the cross-derivative discretization. Furthermore, the matrices A_1 and A_2 share evenly the discretization of the u (no-derivative) term in (2).

For the parabolic PDE (2) to be well-posed, we assume that the symmetric matrix arising from the coefficients is positive definite, and that appropriate initial and boundary conditions are given. For the timestepping, we present the standard θ -timestepping method, and the ADI-DR and ADI-MCS methods, described next.

3.2. θ -timestepping. Let θ be such that $0 \leq \theta \leq 1$. To proceed from time τ^{k-1} to time τ^k , with stepsize $\Delta\tau^k = \tau^k - \tau^{k-1}$, the θ -timestepping discretization scheme to (2) solves the linear system

$$(12) \quad (I - \theta(\Delta\tau^k)A)\mathbf{u}^k = (I + (1 - \theta)(\Delta\tau^k)A)\mathbf{u}^{k-1} + (\Delta\tau^k)(\theta\mathbf{g}^k + (1 - \theta)\mathbf{g}^{k-1})$$

where I is the identity matrix of order $(N_x - 1)(N_y - 1)$, and \mathbf{g}^k is a vector of size $(N_x - 1)(N_y - 1)$, containing contributions from the boundary conditions at τ^k .

In (12), the values $\theta = 1/2$ and $\theta = 1$ give rise to the standard Crank-Nicolson (CN) and the fully-implicit (Backward Euler - BE) methods, respectively. It is known that the CN method is second-order accurate, but prone to producing spurious oscillations, while BE is first order accurate, but exhibits stronger stability properties (e.g. [19]). For the BS equation with the non-smooth initial condition (3), to maintain the accuracy of CN as well as the effect of stronger stability of BE, the *Rannacher smoothing* technique [20], which applies the fully-implicit timestepping in the first few timesteps, using a smaller time stepsize, then switches to CN was used. While several other smoothing techniques have been suggested, for example, [16], [21], the Rannacher smoothing is widely used by several researchers; see, for example, [8].

3.3. ADI-DR/ADI-MCS timestepping. Alternating Direction Implicit methods are efficient implicit methods for solving D -dimensional parabolic PDEs, with $D \geq 2$.

A way to present ADI methods for problem (2) is to consider the semi-discretized form of the problem after the spatial derivatives are discretized by FDs, which is

written as an initial value problem for a system of ODEs,

$$(13) \quad u'(\tau) = F(\tau, u(\tau)) \quad (\tau \geq 0) \quad u(0) = u^*$$

where u^* is the initial vector, and F is a given vector-valued function which can be split into the sum

$$(14) \quad F(\tau, v) = F_0(\tau, v) + F_1(\tau, v) + F_2(\tau, v).$$

The term F_0 contains all contributions to F stemming from the mixed derivative terms in (2) and it is treated explicitly in the numerical time-integration. The terms F_1 and F_2 represent the contribution to F stemming from the first- and second-order derivatives in the s_1 and s_2 -directions, respectively. These terms are treated implicitly, at appropriate substeps of the method. The u term, i.e. the no-derivative term, is distributed evenly among the F_1 and F_2 terms.

One of the ADI methods considered in this paper is known as Douglas and Rachford (DR) method [6], [7], initially introduced for the heat equation. We consider a generalization of the method as presented in [11]. For a two-dimensional problem, the method computes u^k , given u^{k-1} and stepsize $\Delta\tau^k$ as follows:

Douglas and Rachford (DR):

$$(15) \quad \begin{cases} Y_0 = u^{k-1} + (\Delta\tau^k)F(\tau^{k-1}, u^{k-1}), \\ Y_j = Y_{j-1} + \theta(\Delta\tau^k)(F_j(\tau^k, Y_j) - F_j(\tau^{k-1}, u^{k-1})), \quad j = 1, 2 \\ u^k = Y_2. \end{cases}$$

The forward Euler predictor step is followed by two implicit but unidirectional corrector steps, whose purpose is to stabilize the predictor step. We also consider the Modified Craig-Sneyd (MCS) scheme in [12] which computes u^k , given u^{k-1} and stepsize $\Delta\tau^k$ as follows:

Modified Craig-Sneyd (MCS):

$$(16) \quad \begin{cases} Y_0 = u^{k-1} + (\Delta\tau^k)F(\tau^{k-1}, u^{k-1}), \\ Y_j = Y_{j-1} + \theta(\Delta\tau^k)(F_j(\tau^k, Y_j) - F_j(\tau^{k-1}, u^{k-1})), \quad j = 1, 2 \\ \hat{Y}_0 = Y_0 + \sigma(\Delta\tau^k)(F_0(\tau^k, Y_2) - F_0(\tau^{k-1}, u^{k-1})), \\ \hat{Y}_0 = \hat{Y}_0 + \mu(\Delta\tau^k)(F(\tau^k, Y_2) - F(\tau^{k-1}, u^{k-1})), \\ \hat{Y}_j = \hat{Y}_{j-1} + \theta(\Delta\tau^k)(F_j(\tau^k, \hat{Y}_j) - F_j(\tau^{k-1}, u^{k-1})), \quad j = 1, 2 \\ u^k = \hat{Y}_2. \end{cases}$$

The real parameters $\mu, \theta > 0$ and $\sigma > 0$ control the stability and accuracy properties of the method. The MCS method starts with a forward Euler equation predictor, followed by two phases of two implicit unidirectional relations as correctors, the two phases being separated by two explicit relations. Based on previous studies [12], MCS applied to a two-dimensional problem is stable for $\theta \geq \frac{1}{3}$ and has consistency order of 2 if and only if $\{\sigma = \theta, \mu = \frac{1}{2} - \theta\}$. The order of convergence of the MCS method is studied in [13] and is shown to be two with respect to the time stepsize, independently of the spatial mesh width. In [24], the convergence of the MCS scheme combined with Rannacher smoothing and second order FD space discretization is studied for nonsmooth initial data.

For the two-dimensional BS equation (2), and the spatial discretization discussed in Section 3.1, the spatial discretization of $F_i(\tau, u^k)$ gives rise to $A_i u^k + R_i$, $i = 0, \dots, 2$ and $F(\tau, u^k)$ gives rise to $Au^k + R = \sum_{i=0}^2 (A_i u^k + R_i)$, where $A = \sum_{i=0}^2 A_i$, $R = \sum_{i=0}^2 R_i$. Here, $A_i, i = 0, 1, 2$, are discretization matrices of order $(N_x - 1)(N_y - 1)$ corresponding to the continuous $F_i, i = 0, 1, 2$, functions, respectively, and the vectors $R_i, i = 0, 1, 2$, include contributions from the boundaries.

With the matrices A_i and the vectors R_i , we can present the vector/matrix version of the ADI methods. For brevity, and since the ADI-DR method matches with the first few steps of the ADI-MCS method, we include only the ADI-MCS method description. We emphasize that u^* and Y_* denote vectors of values at the grid points of the semi-discrete functions u^* and Y_* , respectively.

Modified Craig-Sneyd (MCS) method in vector/matrix form:

$$(17) \quad \left\{ \begin{array}{l} \text{compute} \quad Y_0 = u^{k-1} + (\Delta\tau^k)(Au^{k-1} + R^{k-1}) \\ \text{solve} \quad (I - \theta(\Delta\tau^k)A_1)Y_1 = Y_0 + \theta(\Delta\tau^k)(R_1^k - A_1u^{k-1} - R_1^{k-1}) \\ \text{solve} \quad (I - \theta(\Delta\tau^k)A_2)Y_2 = Y_1 + \theta(\Delta\tau^k)(R_2^k - A_2u^{k-1} - R_2^{k-1}) \\ \text{compute} \quad \tilde{Y}_0 = Y_0 + \sigma(\Delta\tau^k)(A_0Y_2 + R_0^k - A_0u^{k-1} - R_0^{k-1}) \\ \text{compute} \quad \hat{Y}_0 = \tilde{Y}_0 + \mu(\Delta\tau^k)(AY_2 + R^k - Au^{k-1} - R^{k-1}) \\ \text{solve} \quad (I - \theta(\Delta\tau^k)A_1)\hat{Y}_1 = \hat{Y}_0 + \theta(\Delta\tau^k)(R_1^k - A_1u^{k-1} - R_1^{k-1}) \\ \text{solve} \quad (I - \theta(\Delta\tau^k)A_2)\hat{Y}_2 = \hat{Y}_1 + \theta(\Delta\tau^k)(R_2^k - A_2u^{k-1} - R_2^{k-1}) \\ \text{set} \quad u^k = \hat{Y}_2. \end{array} \right.$$

4. American Spread Options

The price of the American option is greater than its European counterpart, because it gives the holder the right to exercise at any point in time prior to the expiry date. Therefore, the BS model for the American options is more complex and takes the form of a free-boundary problem [23], which can be written as a linear complementarity problem (LCP) as

$$(18) \quad \left\{ \begin{array}{l} \frac{\partial u}{\partial \tau} - Lu > 0 \\ u - u^* = 0 \end{array} \right\} \quad \text{or} \quad \left\{ \begin{array}{l} \frac{\partial u}{\partial \tau} - Lu = 0 \\ u - u^* \geq 0 \end{array} \right\}$$

subject to payoff (3) and appropriate boundary conditions.

Following [8], we replace the LCP (18) by a non-linear PDE obtained by adding a penalty term to the right side of BS equation. More specifically, with a penalty parameter p , $p \rightarrow \infty$, the non-linear PDE considered for pricing an American put option is

$$(19) \quad \frac{\partial u}{\partial \tau} - Lu = p \max(u^* - u, 0)$$

subject to payoff (3) and appropriate boundary conditions. The discretization of (19) is the same as that of (2), as far as the spatial discretization and the timestepping methods are concerned. The only difference is the treatment of the penalty term $p \max(u^* - u, 0)$. The penalty term is discretized as $P^k \cdot (u^* - u^k)$, where u^* is the vector of payoff values and $P^k = P(u^k)$ is a diagonal matrix defined by

$$(20) \quad P_{i_1, i_2}^k \equiv \left\{ \begin{array}{l} p \text{ if } i_1 = i_2 \text{ and } u_{i_1}^k < u_{i_1}^* \\ 0 \text{ otherwise.} \end{array} \right\}$$

Note that P^k depends on u^k , thus there is non-linearity in $P^k \cdot (u^* - u^k)$. To handle the non-linearity, a penalty iteration is introduced at each timestep.

4.1. Penalty iteration for θ -timestepping. Adding the discretized penalty term to (12), gives rise to the linear system

$$(21) \quad \begin{aligned} & (I - \theta(\Delta\tau^k)A)u^k + P^k u^k \\ & = (I + (1 - \theta)(\Delta\tau^k)A)u^{k-1} + (\Delta\tau^k)(\theta g^k + (1 - \theta)g^{k-1}) + P^k u^*. \end{aligned}$$

For convenience, let

$$(22) \quad \mathbf{b}^k \equiv (I + (1 - \theta)(\Delta\tau^k)A)u^{k-1} + (\Delta\tau^k)(\theta\mathbf{g}^k + (1 - \theta)\mathbf{g}^{k-1}).$$

In order to resolve the non-linearity between P^k and u^k , we use the penalty iteration as described in [8]. Let m be the index of the non-linear penalty iteration. Let $u^{k,m}$ be the m th estimate of u^k , and $P^{k,m}$ be the m th penalty matrix constructed at the k th timestep. The initial guess vector $u^{k,0}$ is chosen to be u^{k-1} , i.e. the solution vector at the previous timestep. For convenience, let $u_{i,j}^{k,m}$ denote the component of $u^{k,m}$ corresponding to the $(s_{1,i}, s_{2,j})$ point. Let also tol be a tolerance, usually set to $1/p$. The penalty iteration algorithm for θ -timestepping is described below.

Algorithm 1: Penalty iteration for θ -timestepping to compute u^k given u^{k-1}

1. initialize $u^{k,0} = u^{k-1}$ and compute $P^{k,0} = P(u^{k-1})$ using (20)
2. for $m = 1, \dots$
3. solve $(I - \theta(\Delta\tau^k)A + P^{k,m-1})u^{k,m} = \mathbf{b}^k + P^{k,m-1}u^*$
4. compute $P^{k,m} = P(u^{k,m})$ using (20)
5. if $\max_{i,j} \left\{ \frac{|u_{i,j}^{k,m} - u_{i,j}^{k,m-1}|}{\max\{1, |u_{i,j}^{k,m}|\}} \right\} < tol$ or $P^{k,m} = P^{k,m-1}$, break, endif
6. endfor
7. set $u^k = u^{k,m}$

4.2. Penalty iteration for ADI-MCS timestepping. We introduce the penalty matrix into the MCS method, by introducing it into the solution of the linear system for \hat{Y}_2 , i.e. the last linear system to be solved in the given timestep. An alternative is to introduce the penalty matrix into the solution of the linear systems for Y_2 and \hat{Y}_2 . Our experiments show that both alternatives produce very similar results, and since the former is more efficient, we present only that. Thus, using vector and matrix notation, the penalty iteration algorithm for ADI-MCS timestepping is:

Algorithm 2: Penalty iteration for ADI-MCS timestepping to compute u^k given u^{k-1}

1. initialize $u^{k,0} = u^{k-1}$ and compute $P^{k,0} = P(u^{k-1})$ using (20)
2. compute $Y_0 = u^{k-1} + (\Delta\tau^k)(Au^{k-1} + R^{k-1})$
3. solve $(I - \theta(\Delta\tau^k)A_1)Y_1 = Y_0 + \theta(\Delta\tau^k)(R_1^k - A_1u^{k-1} - R_1^{k-1})$
4. solve $(I - \theta(\Delta\tau^k)A_2)Y_2 = Y_1 + \theta(\Delta\tau^k)(R_2^k - A_2u^{k-1} - R_2^{k-1})$
5. compute $\tilde{Y}_0 = Y_0 + \sigma(\Delta\tau^k)(A_0Y_2 + R_0^k - A_0u^{k-1} - R_0^{k-1})$
6. compute $\hat{Y}_0 = \tilde{Y}_0 + \mu(\Delta\tau^k)(AY_2 + R^k - Au^{k-1} - R^{k-1})$
7. solve $(I - \theta(\Delta\tau^k)A_1)\hat{Y}_1 = \hat{Y}_0 + \theta(\Delta\tau^k)(R_1^k - A_1u^{k-1} - R_1^{k-1})$
8. for $m = 1, \dots$
9. solve $(I - \theta(\Delta\tau^k)A_2 + P^{k,m-1})u^{k,m} = \hat{Y}_1 + \theta(\Delta\tau^k)(R_2^k - A_2u^{k-1} - R_2^{k-1}) + P^{k,m-1}u^*$
10. compute $P^{k,m} = P(u^{k,m})$ using (20)
11. if $\max_{i,j} \left\{ \frac{|u_{i,j}^{k,m} - u_{i,j}^{k,m-1}|}{\max\{1, |u_{i,j}^{k,m}|\}} \right\} < tol$ or $P^{k,m} = P^{k,m-1}$, break, endif
12. endfor
13. set $u^k = u^{k,m}$

Note that, while the MCS method (17) requires the solution of four tridiagonal systems of size $N \times N$ (two for each of the two dimensions of (2)) at each timestep, where $N = (N_x - 1)(N_y - 1)$, each penalty iteration requires the solution of only one tridiagonal system of size $N \times N$ (Line 9 of Algorithm 2), after computing

the solution of three tridiagonal systems of size $N \times N$ outside the iteration loop. Thus the number of tridiagonal solutions at the k th timestep of MCS with penalty iteration is $3 + nit_k$, where nit_k is the number of penalty iterations in the k th timestep. Note that the above ADI-MCS penalty technique is *implicit*, just as the method proposed in [8] for θ -timestepping, and different from the method in [9]. An extensive numerical study of the convergence of various techniques for handling the early exercise boundary of American options is found in [14]. It is also worth noting, that our technique of incorporating the ADI-MCS method into the discrete penalty iteration method for two-dimensional problems, can easily be extended to higher dimensional problems. For example, for a D -dimensional problem, the MCS method (for the linear problem) requires the solution of $2D$ tridiagonal systems of size $N \times N$ at each timestep, while, with the penalty iteration technique (for the nonlinear problem), it requires $2D - 1 + nit_k$ solutions of tridiagonal systems, at each timestep.

5. Numerical Results

Table 1 displays the parameter values of the test cases we considered. In Table 1, s_1^* and s_2^* are points of evaluations. For all cases, the right boundaries are set to $S_1 = 8s_1^*$ and $S_2 = 8s_2^*$. The test cases starting with *EC*, *AC* and *AP* denote European Call, American Call and American Put problems, respectively. Most of the parameter values for the *EC* and *AC* problems are taken from example 3 in [18], and we vary some of these parameters, in order to better study the behaviour of our method. For the *EC* problems, we vary the strike; Problem *AC-P₁* has the same parameter values as *EC-P₁*, and, for this no dividend case, the American and the European call spread options are expected to have the same price; Problem *AC-P₂* is the same as *AC-P₁*, with the exception of non-zero dividends. Most of the parameter values for the *AP* problems are taken from example 2 in [18], and we vary some of these parameters, in order to better study the behaviour of our method. In Problem *AP-P₂*, we increase the correlation level compared to *AP-P₁*, and in problem *AP-P₃*, we also increase the maturity time.

We present results from two instances of our ADI-MCS method, one using uniform (MCS_u), and another using non-uniform (MCS_nu) space grid. In the non-uniform implementation, for each of the two spatial dimensions, we concentrate more points around the respective coordinate of the evaluation point, using the smooth mapping function of uniform to non-uniform points (see [3], [2])

$$(23) \quad f(s) = \left(1 + \frac{\sinh(b(s-a))}{\sinh(ba)}\right)K,$$

with $a \approx 0.38$, and adjusted so that the strike falls on a gridpoint, and b chosen so that the last gridpoint falls exactly at the right boundary. We used $\theta = 1$, $\sigma = \theta$, $\mu = 0.5 - \theta$ for the MCS parameters, and $p = 10^{-5}$ for the penalty parameter.

We compare the ADI-MCS results, whenever appropriate, with the results derived using various other methods, such as other PDE approximation methods, analytical formulae, or MC simulations. More specifically, for comparison purposes, we use the PDE ADI-DR method of MATLAB [7], [5] (FD_Mat, function *spreadsensbyfd*), applicable to both European and American spread options, MATLAB's MC simulations (MC_Matlab, function *spreadsensbyls*), also applicable to both European and American spread options, Margrabe's formula [17] applicable only to European exchange options and giving the exact value, and the analytical approximations by Kirk (Kirk_apprx) [15] and Venkatramanan and Alexander (VenAlex_apprx) [22], applicable only to European spread options (or American call

TABLE 1. Points of evaluation and parameters used in the Black-Scholes equations

Problem	s_1^*	s_2^*	K	T	r	σ_1	σ_2	ρ	q_1	q_2
EC_P_0	105.84	101.61	0	61/365	0.035	0.38	0.34	0.35	0	0
EC_P_1	105.84	101.61	4.5	61/365	0.035	0.38	0.34	0.35	0	0
EC_P_2	105.84	101.61	7.0	61/365	0.035	0.38	0.34	0.35	0	0
AC_P_1	105.84	101.61	4.5	61/365	0.035	0.38	0.34	0.35	0	0
AC_P_2	105.84	101.61	4.5	61/365	0.035	0.38	0.34	0.35	0.0762	0.1169
AP_P_1	127.68	99.43	25	61/365	0.035	0.35	0.38	0.30	0	0
AP_P_2	127.68	99.43	25	61/365	0.035	0.35	0.38	0.60	0	0
AP_P_3	127.68	99.43	25	122/365	0.035	0.35	0.38	0.60	0	0

spread options with zero dividends). The FD_Mat results presented are for the same grid resolutions as the MCS_u and MCS_nu results. It is worth noting that MATLAB's *spreadsensbyfd* (FD_Mat) applies a logarithmic transformation to the s_i variables, then discretizes them on a uniform grid. For the MC_Matlab results, we run 100,000 paths, and used 1/365 as stepsize, for both European and American cases. Note that, for the American case, the function *spreadsensbyls* automatically sets the stepsize to 1/365. The Margrabe, Kirk_aprx and VenAlex_aprx formulae are continuous functions and do not have discretization parameters. We emphasize that, of all these methods, only Margrabe's formula is exact.

In Table 2, we present results from the *EC* problems EC_P_0 and EC_P_2 , obtained by FD_Mat, MCS_u and MCS_nu PDE approximation methods. Furthermore, we present results from MC_Matlab, Margrabe (for EC_P_0) and Kirk_aprx and VenAlex_aprx (for EC_P_2). Since the prices of European and American call spread options with zero dividends are the same, we just mention that our numerical results also agree with this fact, and, for brevity, we omit the results for EC_P_1 , as they are similar to the ones of AC_P_1 , presented later. The results of Table 2 indicate reasonable agreement between the analytical formulae, MC simulations, and all PDE discretization methods, with the MCS_nu method being the closest to Margrabe for EC_P_0 and to Kirk for EC_P_2 . We also notice full monotonic convergence for MCS_nu, while monotonic convergence for MCS_u and FD_Mat is missed only in a few coarse grid cases, but asymptotically still observed. Furthermore, comparing the values from EC_P_0 and EC_P_2 , we notice that the spread call option value decreases as the strike increases, which is expected, as a larger strike reduces the payoff.

In Table 3, we present results from the *AC* problems, obtained by the FD_Mat, MCS_u and MCS_nu PDE approximation methods. Furthermore, we present results from MC_Matlab. For AC_P_1 , we also show the values of Kirk_aprx and VenAlex_aprx, since these formulae, designed for European spread options, are applicable to zero dividend American call options too. Furthermore, in Table 3, we list the number of penalty iterations, only for the MCS_nu method, as the number of penalty iterations for MCS_u were very similar to those of MCS_nu.

For AC_P_1 , we again notice reasonable agreement between the analytical formulae, MC simulations, and all PDE discretization methods, with the MCS_nu method being the closest to Kirk for AC_P_1 (EC_P_1). We also notice monotonic convergence for MCS_nu and FD_Mat. When comparing the results of AC_P_1 (EC_P_1) and EC_P_2 , we notice that Kirk_aprx deviates from MCS_nu more as the strike increases. If we assume that our MCS_nu results with large grids give the most

TABLE 2. Prices at (s_1^*, s_2^*) of three numerical PDE methods with various grid sizes for EC_P_0 and EC_P_2 . For comparison, for EC_P_0 , Margrabe (exact) = 9.2753426. For EC_P_2 , Kirk_apprx = 5.7273001, VenAlex_apprx = 5.6950133, and MC_Matlab = 5.6998858.

Problem $N_x \times N_y \times N_t$	EC_P_0			EC_P_2		
	FD_Mat	MCS_u	MCS_nu	FD_Mat	MCS_u	MCS_nu
$32 \times 16 \times 61$	9.574830	8.597333	9.122241	6.139433	4.640012	5.589742
$64 \times 32 \times 122$	9.645158	9.431610	9.257059	6.068464	5.772938	5.708169
$128 \times 64 \times 244$	9.312788	9.352157	9.271836	5.761532	5.812146	5.723239
$256 \times 128 \times 488$	9.300076	9.292630	9.274627	5.750488	5.736627	5.725557
$512 \times 256 \times 976$	9.280919	9.279982	9.275167	5.731687	5.730293	5.726053

TABLE 3. Prices at (s_1^*, s_2^*) of three numerical methods and number of penalty iterations (p. it) with various grid sizes for AC_P_1 and AC_P_2 . For comparison, for AC_P_1 , Kirk_apprx = 6.8656070, VenAlex_apprx = 6.8242103, while MC_Matlab = 6.8589669. For AC_P_2 , MC_Matlab = 7.0777440.

Problem $N_x \times N_y \times N_t$	AC_P_1			
	FD_Mat	MCS_u	MCS_nu	p. it
$32 \times 16 \times 61$	7.362621	5.075992	6.723185	130
$64 \times 32 \times 122$	7.238465	6.650605	6.848179	255
$128 \times 64 \times 244$	6.905050	6.885889	6.862544	528
$256 \times 128 \times 488$	6.891098	6.881371	6.864935	1060
$512 \times 256 \times 976$	6.871178	6.871348	6.865274	2023
Problem $N_x \times N_y \times N_t$	AC_P_2			
	FD_Mat	MCS_u	MCS_nu	p. it
$32 \times 16 \times 61$	7.512371	5.361243	6.927942	125
$64 \times 32 \times 122$	7.421661	6.890148	7.052129	258
$128 \times 64 \times 244$	7.103625	7.096546	7.066011	527
$256 \times 128 \times 488$	7.093056	7.086801	7.068371	1052
$512 \times 256 \times 976$	7.074242	7.075286	7.068662	2021

accurate prices, and take into account that, according to [15], the closed-form approximation become less accurate as the strike price grows larger compared to s_2^* , then the increase of deviation of Kirk_apprx with the increase in strike is expected. For AC_P_2 , we again notice reasonable agreement between MC simulations, and all PDE discretization methods. When comparing the results of AC_P_1 and AC_P_2 , we notice that the larger dividend for s_2 results in larger price for the option. This is expected, since the larger dividend for s_2 increases the spread, and thus the payoff of the option.

Looking at the total number of penalty iterations in Table 3, we can easily find that the average number of penalty iterations for MCS varies between 2.05 and 2.20, and, for the finest grids, it is 2.07. The small variance in number of iterations indicates that the convergence rate of penalty iteration is independent of the problem size. Note that the computation of the first penalty iteration is attributed to the plain MCS method, therefore, essentially only one penalty iteration suffices to obtain convergence.

In Tables 4 and 5, we present results from the AP problems, obtained by the FD_Mat, MCS_u and MCS_nu PDE approximation methods. For AP_P_1 , we also

TABLE 4. Prices at (s_1^*, s_2^*) and number of penalty iterations (p. it) of four numerical methods with various grid sizes for AP_P_1 . For comparison, MC_Matlab = 6.42514245.

$N_x \times N_y \times N_t$	FD_Mat	MCS_u	MCS_nu	p. it	CN_nu	p. it
$32 \times 16 \times 61$	7.537957	5.023413	6.244111	134	6.246340	141
$64 \times 32 \times 122$	6.758517	6.378849	6.382559	269	6.382566	303
$128 \times 64 \times 244$	6.491617	6.432238	6.398929	540	6.398665	552
$256 \times 128 \times 488$	6.416549	6.414472	6.401766	1033	6.401568	1031
$512 \times 256 \times 976$	6.407908	6.405585	6.402309	2005	6.402195	1996

TABLE 5. Prices at (s_1^*, s_2^*) and number of penalty iterations (p. it) of three numerical methods with various grid sizes for AP_P_2 and AP_P_3 . For comparison, for AP_P_2 , MC_Matlab = 4.5322051, and for AP_P_3 , MC_Matlab = 6.9451714.

Problem	AP_P_2			
$N_x \times N_y \times N_t$	FD_Mat	MCS_u	MCS_nu	p. it
$32 \times 16 \times 61$	6.326957	4.277741	4.524914	131
$64 \times 32 \times 122$	5.185030	5.166896	4.542905	260
$128 \times 64 \times 244$	4.716645	4.865245	4.531880	527
$256 \times 128 \times 488$	4.565280	4.654163	4.527039	1100
$512 \times 256 \times 976$	4.537528	4.564074	4.525580	2124
Problem	AP_P_3			
$N_x \times N_y \times N_t$	FD_Mat	MCS_u	MCS_nu	p. it
$32 \times 16 \times 122$	8.371589	7.277957	6.941974	232
$64 \times 32 \times 244$	7.538642	7.677932	6.956781	504
$128 \times 64 \times 488$	7.073126	7.243086	6.941153	1015
$256 \times 128 \times 976$	6.973622	7.038208	6.934672	2076
$512 \times 256 \times 1952$	6.942077	6.962628	6.932875	4076

present results by the CN timestepping method. For brevity, we only include the non-uniform grid CN results (CN_nu). Furthermore, we present results from MC_Matlab. We also list the number of penalty iterations, for brevity, only for the MCS_nu and CN_nu methods. Notice that Problem AP_P_3 has double maturity time, and we used double the number of timesteps. For AP_P_1 , all PDE discretization methods exhibit monotonic convergence, except one coarse grid case of MCS_u. The average number of penalty iterations is around 2 for both MCS_nu and CN_nu. For AP_P_2 and AP_P_3 , where the correlation value is larger, the monotonic convergence is disturbed for the coarse grid sizes, but recovered for the fine ones. As explained in [4], the standard tensor-product centered cross-derivative FD approximation may hinder the monotonicity properties of the matrix to be solved, and when this term comes with a larger factor (larger ρ), it becomes more prominent. However, as discussed later in the experimental convergence study, the convergence order of the PDE methods is still almost 2. Furthermore, the average number of penalty iterations per timestep remains approximately 2, i.e. one extra tridiagonal solution is needed per timestep for MCS, besides the four tridiagonal solutions of the main MCS method.

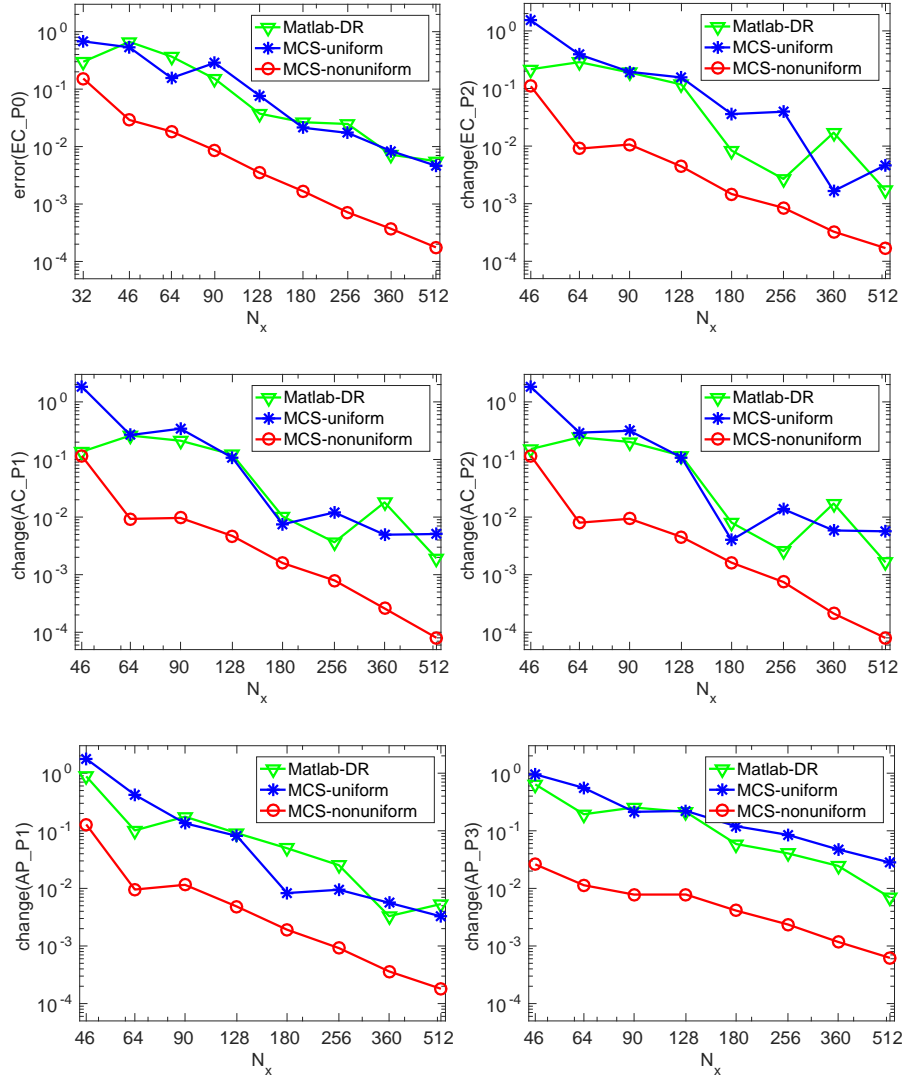


FIGURE 1. Log-log scale graphs of the error or change vs. grid size N_x for different test case problems.

We next present an experimental study of the convergence of the three PDE approximation methods, `FD_Mat`, `MCS_u` and `MCS_nu`. For European exchange (zero strike spread) options, i.e. Problem EC_{P0} , Margrabe's formula [17] gives the exact value, so we can calculate the exact error for any approximation method. For European spread options (with non-zero strike), there is no exact formula. We emphasize that PDE approximation methods exhibit the property of converging to the solution as the discretization is refined and more computational power is utilized, with the convergence being limited mainly by the machine precision. The analytical approximations do not possess this property. They are of more limited accuracy, and, therefore, we do not expect the PDE discretization methods to asymptotically converge to any of the analytical approximations, such as `Kirk_apprx` or `VenAlex_apprx`. Computing the error as the difference of a numerical solution

TABLE 6. Maximum and mean changes at several points about 20% away of (s_1^*, s_2^*) , as compared to FD_Mat changes at (s_1^*, s_2^*) , for problem AP_P_1 .

$N_x \times N_y \times N_t$	FD_Mat		MCS_nu			
	change	order	max	order	mean	order
$64 \times 32 \times 122$	7.8e-01		2.8e-02		1.2e-02	
$128 \times 64 \times 244$	2.7e-01	1.55	1.6e-02	0.81	5.7e-03	1.07
$256 \times 128 \times 488$	7.5e-02	1.83	3.1e-03	2.37	1.1e-03	2.37
$512 \times 256 \times 976$	8.6e-03	3.12	6.4e-04	2.28	2.3e-04	2.26

from another state of-the-art numerical method or a closed form approximation carries the problem that we are not guaranteed that the reference solution is more accurate than our numerical solution.

Considering this, for all the test cases except European exchange options, the error at a particular grid resolution is estimated by the difference (change) of the solution value with that grid resolution from the solution value with the previous (coarser) grid resolution.

For brevity, we do not list the errors or changes, but present plots that indicate the behaviour of the methods. In the graphs of Figure 1, we plot, in log-log scale, the error or change corresponding to Problems EC_P_0 , EC_P_2 , AC_P_1 , AC_P_2 , AP_P_1 and AP_P_3 , for the methods FD_Mat, MCS_u and MCS_nu. In the plots, we included more grid sizes than in the tables, in order to gain better insight on the behaviour of the methods. We notice that MCS_nu exhibits a stable order of convergence (easily calculated from the results of the tables to be close to 2), and the least error (or change) compared to the other PDE approximation methods. More specifically, the MCS_nu error or change is about one order lower than that of the other methods. Furthermore, the FD_Mat and MCS_u errors fluctuate a bit, even for some large grids.

For AP_P_1 , we also consider the prices at several grid points in a rectangular area that extends 20% in each direction around the original evaluation point. In Table 6, we report the maximum and mean value changes on a 5×5 grid of points in this area, i.e. 25 points. These points are not necessarily points of the discretization grid. In order to calculate the prices at the 25 points, we use the MATLAB *interp2* function, to carry two-dimensional spline interpolation. Table 6, also presents the FD_Mat price changes at the single evaluation point, and the orders of convergence of the displayed changes. We notice that the MCS_nu max (and mean) changes are still significantly smaller than the FD_Mat changes on just the single evaluation point, and the orders remain close to 2.

Table 7 displays values of Greeks, in particular, values of $\Delta_1 = \partial u / \partial s_1$, $\Delta_2 = \partial u / \partial s_2$, $\Gamma_1 = \partial^2 u / \partial s_1^2$, and $\Gamma_2 = \partial^2 u / \partial s_2^2$ obtained by MCS_nu for different mesh sizes and allows us to compare them with the FD_Mat results as well as results from MC simulations. For brevity, we did not include the MCS_u values of Greeks. However, in Figure 2, we plot the changes of Greeks for FD_Mat, MCS_u and MCS_nu, versus the grid size, including more data than in Table 7. The Greeks obtained by MCS_nu exhibit monotonic convergence (except one coarse grid Δ_1 case). The orders of convergence of the changes for MCS_nu can be easily calculated from the data and are approximately 2 and fairly stable, as the grid is refined. MCS_u exhibits almost similar convergence order behaviour as MCS_nu, with some fluctuations only for the coarse grids, while the MCS_u changes are about one or two orders

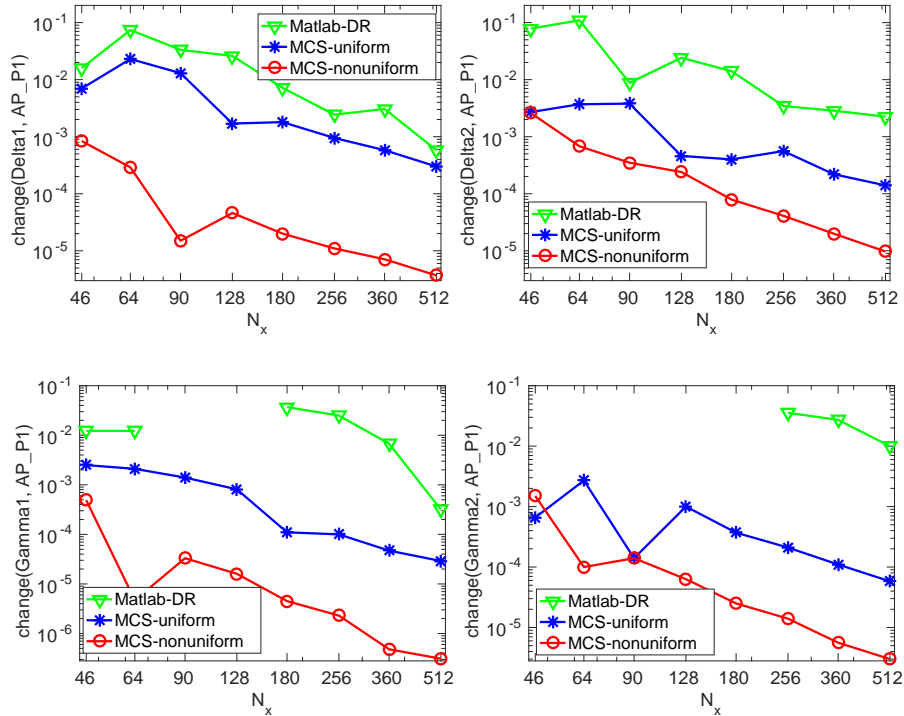


FIGURE 2. Log-log scale graphs of the change vs. grid size N_x for Delta and Gamma values of problem AP_{P1} .

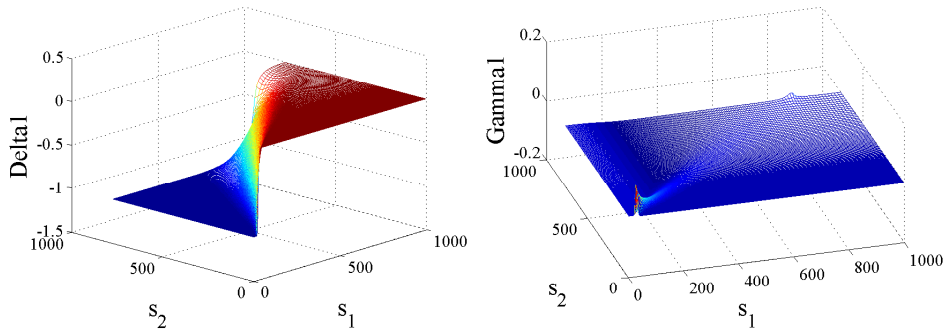


FIGURE 3. The Greeks Δ_1 (left) and Γ_1 (right) calculated for problem AP_{P1} , solved by the MCS_nu method.

higher than those of MCS_nu. The Greeks obtained by FD_Mat do not converge monotonically, but, most importantly, some of the values obtained do not have any correct digits. The convergence orders of the changes for FD_Mat, whenever they can be calculated, are fluctuating. These results indicate the MCS_nu is substantially more reliable method for computing the Greeks than FD_Mat, with MCS_u being reliable, but less accurate than MCS_nu. Figure 3 gives three-dimensional plots of Δ_1 (left) and Γ_1 (right) for problem AP_{P1} calculated by the MCS_nu method.

TABLE 7. Delta and Gamma values at point (s_1^*, s_2^*) for AP_P_1 . For comparison, $MC_Matlab(\Delta_1) = -0.405427490$, $MC_Matlab(\Delta_2) = 0.477727230$, $MC_Matlab(\Gamma_1) = 0.044671072$ and $MC_Matlab(\Gamma_2) = 0.038212200$.

$N_x \times N_y \times N_t$	$\Delta_1(\text{FD_Mat})$	$\Delta_1(\text{MCS_nu})$	$\Delta_2(\text{FD_Mat})$	$\Delta_2(\text{MCS_nu})$
$32 \times 16 \times 61$	-0.47619079	-0.40038480	0.50423501	0.46551430
$64 \times 32 \times 122$	-0.38621580	-0.40093240	0.47275222	0.46882980
$128 \times 64 \times 244$	-0.39353201	-0.40090210	0.45739797	0.46942040
$256 \times 128 \times 488$	-0.40316349	-0.40087120	0.46803051	0.46954080
$512 \times 256 \times 976$	-0.40067206	-0.40086030	0.46864958	0.46957030
$N_x \times N_y \times N_t$	$\Gamma_1(\text{FD_Mat})$	$\Gamma_1(\text{MCS_nu})$	$\Gamma_2(\text{FD_Mat})$	$\Gamma_2(\text{MCS_nu})$
$32 \times 16 \times 61$	0.00000000	0.01961120	0.00000000	0.01831630
$64 \times 32 \times 122$	0.00000000	0.01912450	-0.00000000	0.01994320
$128 \times 64 \times 244$	0.00000000	0.01907570	-0.00000000	0.02014250
$256 \times 128 \times 488$	0.01189903	0.01906890	0.03562448	0.02018090
$512 \times 256 \times 976$	0.01833890	0.01906810	0.01834768	0.02018960

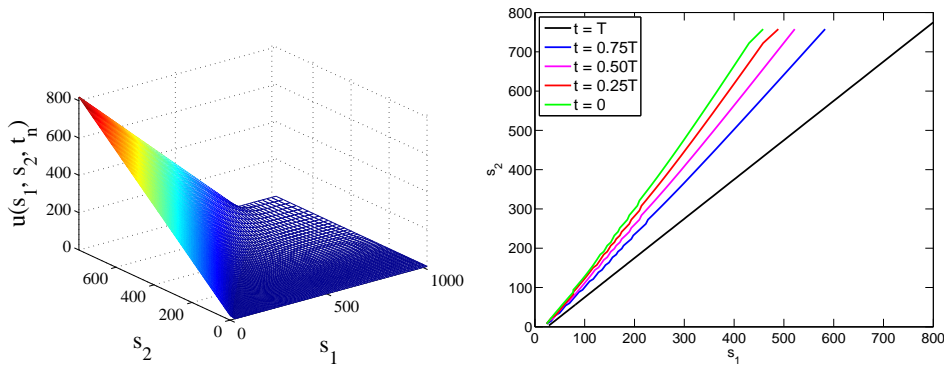


FIGURE 4. The non-uniform MCS approximation of problem AP_P_1 (left) and free boundary lines at different timesteps for problem AP_P_1 (right).

Figure 4 presents a three-dimensional plot of the solution (left) as well as the evolution of the free boundary (right) for problem AP_P_1 solved by the non-uniform MCS method. The free boundary plot shows that, for the case of American spread put options, the free boundary starts ($t = T$ or $\tau = 0$) at the line $K - s_1 + s_2 = 0$, where discontinuity of the first derivatives of the payoff occurs, and, as t goes to 0 (τ goes to T), moves away towards the left.

6. Summary

The pricing of European and American spread options was considered using a two-dimensional Black-Scholes PDE model, solved by an ADI-MCS method. The ADI-MCS method, especially when implemented with a non-uniform grid, is shown to be a competitive timestepping technique for spread option pricing. In the case of American spread options, a penalty iteration technique is proposed for the handling of the early exercise feature. We explain how to bind the penalty iteration technique efficiently with ADI-MCS. The number of tridiagonal system solutions on top of

those of the ADI-MCS method required due to the penalty iteration is essentially one per timestep, irrespectively of grid size. The way we incorporated ADI-MCS into the penalty iteration can be straightforward extended to problems of higher dimensions. Our numerical experiments demonstrate that, for European exchange options, we obtain second order convergence to the exact value given by Margrabe's formula. For other spread options, we obtain second order convergence behavior for price values and the Greeks, as well as smooth solutions, Greeks, and free boundary lines. The ADI-MCS results demonstrate reasonable agreement with those of MC simulations, MATLAB's ADI-DR, as well as with those obtained by Kirk's formula, with the changes of ADI-MCS prices from one grid resolution to a finer one being at least an order smaller than the MATLAB ADI-DR ones, and the changes of ADI-MCS Greeks being several orders smaller than the MATLAB ADI-DR ones.

Acknowledgments

This research was supported by the Natural Sciences and Engineering Research Council of Canada.

References

- [1] Brennan, M. and Schwartz, E., The valuation of the American put option, *J. Finance*, 32 (1977), pp. 449–462.
- [2] Christara, C. C. and Dang, D. M., Adaptive and high-order methods for valuing American options, *J. Comput. Finance*, 14 (2011), pp. 73–113.
- [3] Clarke, N. and Parrott, K., Multigrid for American option pricing with stochastic volatility, *Appl. Math. Finance*, 6 (1999), pp. 177–195.
- [4] Clift, S. S. and Forsyth, P. A., Numerical solution of two asset jump diffusion models for option valuation, *Appl. Numer. Math.*, 58 (2008), pp. 743–782.
- [5] Craig, I. and Sneyd, A., An alternating-direction implicit scheme for parabolic equations with mixed derivatives, *Comp. Math. Appl.*, 16 (1988), pp. 341–350.
- [6] Douglas, J. and Rachford, H., On the numerical solution of heat conduction problems in two and three space variables, *Trans. Amer. Math. Society*, 82 (1956), pp. 421–439.
- [7] Fairweather, G. and Mitchell, A. R., A new computational procedure for A.D.I. methods, *SIAM J. Numer. Anal.*, 4 (1967), pp. 163–170.
- [8] Forsyth, P. A. and Vetzal, K. R., Quadratic convergence for valuing American options using a penalty method, *SIAM J. Sci. Comput.*, 23 (2002), pp. 2095–2122.
- [9] Haentjens, T. and in 't Hout, K. J., ADI schemes for pricing American options under the Heston model, *Appl. Math. Finance*, 22 (2015), pp. 207–237.
- [10] Ikonen, S. and Toivanen, J., Pricing American options using LU decomposition, *Appl. Math. Sci.*, 1 (2007), pp. 2529–2551.
- [11] in 't Hout, K. and Welfert, B., Stability of ADI schemes applied to convection-diffusion equations with mixed derivative terms, *Appl. Numer. Math.*, 57 (2007), pp. 19–35.
- [12] ———, Unconditional stability of second-order ADI schemes applied to multi-dimensional diffusion equations with mixed derivative terms, *Appl. Numer. Math.*, 59 (2009), pp. 677–692.
- [13] in 't Hout, K. and Wyna, M., Convergence of the Modified Craig-Sneyd scheme for two-dimensional convection-diffusion equations with mixed derivative term, *J. Comp. Appl. Math.*, 296 (2016), pp. 170–180.
- [14] in 't Hout, K. J. and Valkov, R. L., Numerical study of splitting methods for American option valuation, in *Novel Methods in Computational Finance*, Ehrhardt, M., Günther, M. and ter Maten, J., eds., Springer, 2017. To appear. Retrieved 17-6-2017, from <https://arxiv.org/pdf/1610.09622.pdf>, pp. 1–21.
- [15] Kirk, E., Correlation in the energy markets, in *Managing Energy Price Risk*, V. Kaminski, ed., vol. 1, Risk Publications, 1995, pp. 71–78.
- [16] Kreiss, H. O., Thomée, V. and Widlund, O., Smoothing of initial data and rates of convergence for parabolic difference equations, *Commun. Pure Appl. Math.*, 23 (1970), pp. 241–259.
- [17] Margrabe, M., The value of an option to exchange one asset for another, *J. Finance*, 33 (1978), pp. 177–186.

- [18] Mathworks, Hedging strategies using spread options (on-line guide). <https://www.mathworks.com/help/fininst/examples/hedging-strategies-using-spread-options.html>, retrieved 5-6-2017.
- [19] Pooley, D. M., Vetzal, K. R. and Forsyth, P. A., Convergence remedies for non-smooth payoffs in option pricing, *J. Comput. Finance*, 6 (2003), pp. 25–40.
- [20] Rannacher. R., Finite element solution of diffusion problems with irregular data, *Numerische Mathematik*, 43 (1984), pp. 309–327.
- [21] Reisinger, C. and Whitley, A., The impact of a natural time change on the convergence of the Crank-Nicolson scheme, *IMA J. Numer. Anal.*, 34 (2014), pp. 1156–1192.
- [22] Venkatramanan, A. and Alexander, C., Closed form approximations for spread options, *Appl. Math. Finance*, 18 (2011), pp. 447–472.
- [23] Wilmott, P., Howison, S. and Dewynne, J., *The Mathematics of Financial Derivatives*, Cambridge University Press, 1995.
- [24] Wyns, M., Convergence analysis of the Modified Craig-Sneyd scheme for two-dimensional convection-diffusion equations with nonsmooth initial data, *IMA J. Numer. Anal.*, 37 (2017), pp. 798–831.

Department of Computer Science, University of Toronto, Toronto, Ontario M5S 3G4, Canada
E-mail: vidahd@cs.toronto.edu and ccc@cs.toronto.edu
URL: <http://www.cs.toronto.edu/~ccc/>